Turkish Journal of Earth Sciences (Turkish J. Earth Sci.), Vol. 17, 2008, pp. 803–819. *Copyright ©TÜBİTAK*
First published online 13 March 2008

On the Origin and Age of the Arıburnu Beachrock, Gelibolu Peninsula, Turkey

AHMET EVREN ERGİNAL[1], NAFİYE GÜNEÇ KIYAK[2], MUSTAFA BOZCU[3], AHMET ERTEK[4], HAKAN GÜNGÜNEŞ[5], ALİ SUNGUR[6] & GÜLEN TÜRKER[7]

[1] Çanakkale Onsekiz Mart University, Department of Geography, TR–17000 Çanakkale, Turkey
(e-mail: aerginal@comu.edu.tr)

[2] Işık University, Department of Physics, Kumbaba Mevkii, Şile, TR–34980 İstanbul, Turkey

[3] Çanakkale Onsekiz Mart University, Department of Geological Engineering, TR–17000 Çanakkale, Turkey

[4] İstanbul University, Department of Geography, Ordu Caddesi, Laleli, TR–34459 İstanbul, Turkey

[5] Hitit University, Department of Physics, Faculty of Science and Art Campus, TR–19030 Çorum, Turkey

[6] Çanakkale Onsekiz Mart University, Department of Soil Science, TR–17000 Çanakkale, Turkey

[7] Çanakkale Onsekiz Mart University, Department of Chemistry, TR–17000 Çanakkale, Turkey

Abstract: The beachrock formation on the Arıburnu coast situated in the Gelibolu Peninsula has been studied by field observation, thin-section interpretation, physicochemical analyses including ICP-AES and SEM/EDS, and OSL dating. These analyses reveal the presence of different amounts of major (Si, Ca, Mg, K, Fe, Al and Na) and trace elements within the beachrock cement with Si (36.2%) and Ca (32.68%) dominating the overall composition. Beachrocks composed of highly-fractured and friable beds reach a total thickness of 80 cm extending from +60 cm at the uppermost level down to –1 m at their most seaward extent and grade from conglomerate to lithic arkose in vertical section. The total amount of $CaCO_3$ ranges between 59.08% and 36% and the cement consists of high-Mg calcite based on EDS analysis. From SEM examination, four main morphologies were identified in cement material: (1) micritic coatings, (2) cryptocrystalline pore-filling cement, (3) meniscus cement and (4) microbial cement and suggest the presence of marine phreatic conditions with the exception of meniscus bridges, which imply that cementation may have been dominated by carbonate-rich meteoric waters at any successive stage of cementation. Five buried beachrock samples under unconsolidated beach sand were sampled for Optically Stimulated Luminescence (OSL) dating and show that the minimum and maximum ages of beachrock are 1.42±0.20 ka and 2.28±0.28 ka BP, respectively.

Key Words: beachrock, carbonate cement, intertidal lithification, diagenesis, Gelibolu Peninsula, Turkey

Arıburnu Yalıtaşının (Gelibolu Yarımadası, Türkiye) Kökeni ve Yaşı Üzerine

Özet: Bu çalışmada Gelibolu Yarımadası'nda, Arıburnu kıyılarındaki yalıtaşı oluşumu arazi verileri, ince kesit yorumlamaları, ICP-AES, EDS ve SEM analizleri ve OSL yaşlandırması ile ele alındı. Analizler yalıtaşı çimentosu içinde Si, Ca, Mg, K, Fe, Al ve Na gibi ana ve iz elementlerin nispeten farklı oranlarda bulunduğunu göstermektedir. Bileşimde Si (36.2%) ve Ca (32.68%) egemendir. Yalıtaşları bol kırıklı ve kırılgan, toplam 80 cm tabaka kalınlığına sahip olup, en yüksek seviyede +60 cm'den deniz içinde –1 m'ye kadar takip edilirler. Düşey kesitte çakıltaşlarından litik arkoza geçişlidirler. Toplam $CaCO_3$ miktarı 59.08% ve 36% arasında değişir. EDS analizlerine gore çimento maddesi yüksek magnezyum kalsittir. SEM analizlerine göre çimento maddesinde 4 ana morfoloji tanımlanmıştır; (1) mikritik tabakalar, (2) kriptokristalin boşluk dolgusu çimento, (3) menisküs çimento ve (4) mikrobial çimento. Bu çimentolar, çimentolanmanın izleyen bir devresinde karbonat bakımından zengin meteorik sularca meydana getirildiğini gösteren menisküs çimento hariç, denizel freatik koşullarda geliştiğini göstermektedir. Kıyı çizgisi gerisindeki plaj kumları altından çıkarılan 5 örneğin '*optik uyarımlı ışınım tekniği (OSL)*' yöntemi ile yaşlandırması yapıldı. Analizler yalıtaşının oluşum yaşı için minimum 1.42±0.20 bin yıl ve maksimum 2.28±0.28 bin yıl yaşlarını vermektedir.

Anahtar Sözcükler: yalıtaşı, karbonat çimento, gelgit içi taşlaşma, diyajenez, Gelibolu Yarımadası, Türkiye

Introduction

Beachrock is a type of sedimentary formation which generally occurs in tropical and subtropical beaches as result of intertidal lithification of loose beach sands and gravels by carbonate cementation (Ginsburg 1953). It is defined as a conglomeratic formation or a layered deposit inclined towards the sea (Bricker 1971; Neumeier 1998). Although most modern beachrocks are restricted to

latitudes lying between 35°N and 35°S (Scoffin & Stoddart 1983), current publications identify its occurrence in different climatic regions of the world including tropical and subtropical beaches with humid or arid-semiarid climate (Ginsburg 1953; Taylor & Illing 1969; Moore 1973; Beier 1985; Neumeier 1998; Webb *et al*. 1999), and the coasts of the Mediterranean Sea (Friedman & Gavish 1971; Alexanderson 1972; Holail & Rashed 1992). These formations have also been found on mid-latitude coasts, such as northwest and west Ireland (Sellwood 1995) and northwest Scotland (Kneale & Viles 2000).

Current debates on beachrock occurrence mostly explain the place where beach clasts amalgamated in terms of a carbonate cement process linked to the high porosity and permeability of sands and gravels (Moore 1989) allowing easy circulation of water. Different theories identify dominant factors governing beachrock cementation including mixing of marine and meteoric water fluxes (Schmalz 1971; Moore 1973), CO_2 degassing of shallow groundwater in the vadose zone (Hanor 1978), accumulation of $CaCO_3$ by evaporation of sea water (Stoddart & Cann 1965; Taylor & Illing 1969; Scoffin 1970; Moore & Billings 1971; Meyers 1987) and biological activity (Krumbein 1979; Webb *et al*. 1999; Neumeier 1999).

Beachrocks are widely observed on the southern and western coasts of Turkey where their occurrence has been a subject of debate since the pioneering work of Admiral Francis Beaufort (1818), who used the term *petrified beach* for the cemented deposits between Datça Peninsula and Gazipaşa district on the Mediterranean coast of Turkey (Avşarcan 1997). Beachrocks from Teke (Spratt & Forbes 1847) and İskenderun Gulf (Goudie 1966) on the southern coast of Turkey have also been reported.

Despite their considerable extent, very little is known about beachrock occurrence along Turkey's coastline whilst recent studies of beachrock strings from the coasts of the Mediterranean Sea (Bener 1974; Erol 1983; Avşarcan 1997), Aegean Sea (Erol 1972; Ertek & Erginal 2003), and Black Sea (Ertek 2001; Turoğlu & Cürebal 2005) have been commonly based upon observational evidence.

The present paper contributes to current debates on beachrock genesis from the west coast of the Gelibolu Peninsula in northwest Turkey and the main objective of this preliminary study is to explain causative factors of cementation and suggest a model for beachrock diagenesis with special emphasis on geomorphologic, petrographic and geochemical characteristics. To this end, we first explain the main morphologic and petrographic characteristics of beachrock exposures and adjacent loose beach sands through sieving analysis and thin-section interpretation. Geochemical compositions of the beachrock ledges are discussed using Energy Dispersive X-Ray Spectroscopy (EDS), Scanning Electron Microscopy (SEM) and Inductively Coupled Plasma-Atomic Emission Spectroscopy (ICP-AES) analysis. To date the beachrock Optically Stimulated Luminescence (OSL) was applied to extracted quartz grains using OSL-SAR protocol.

Study Area

The study area is located 2 km south of the Arıburnu beach on the west coast of NE–SW-trending Gelibolu Peninsula in the northwestern part of Turkey (Figure 1). The beach is about 100 m long and bordered by west-facing steep slopes of the Gelibolu Peninsula. The morphology of the peninsula is characterized by a low plateau with elevations varying between 100 m and 400 m. This plateau cuts Upper Miocene deposits consisting of claystone, pebblestone and limestone (Sümengen & Terlemez 1991). The area is not drained by any major stream, but there are small ephemeral creeks that discharge into the sea near the cemented beach.

The climate of the area is typically Mediterranean with a rainfall regime characterized by maximum and minimum precipitation amounts in winter and summer seasons, respectively (Türkeş 1996). According to meteorological data (DMİ), the annual average precipitation amount is 737.9 mm. Monthly average precipitations range from 11 mm to 140 mm. The average temperature is 15.1 ºC with mean temperatures ranging between 6.7 ºC and 24.6 ºC. The tide amplitude is likely between 0.1 m and 1 m according to the distribution of tidal range on world coasts (Guilcher 1965). However, the study area is a microtidal environment with the tidal range of 30–40 cm, which is a characteristic feature of Mediterranean coasts (Kelletat 2006), and alongshore currents are northwards.

Beachrock beds occur along a sandy and shingle beach with an approximate width of 10 m. The beach is backed by a 3-m-high west-facing sea cliff cut in claystone and pebblestone of Late Miocene age (Figure 2a, b). From the

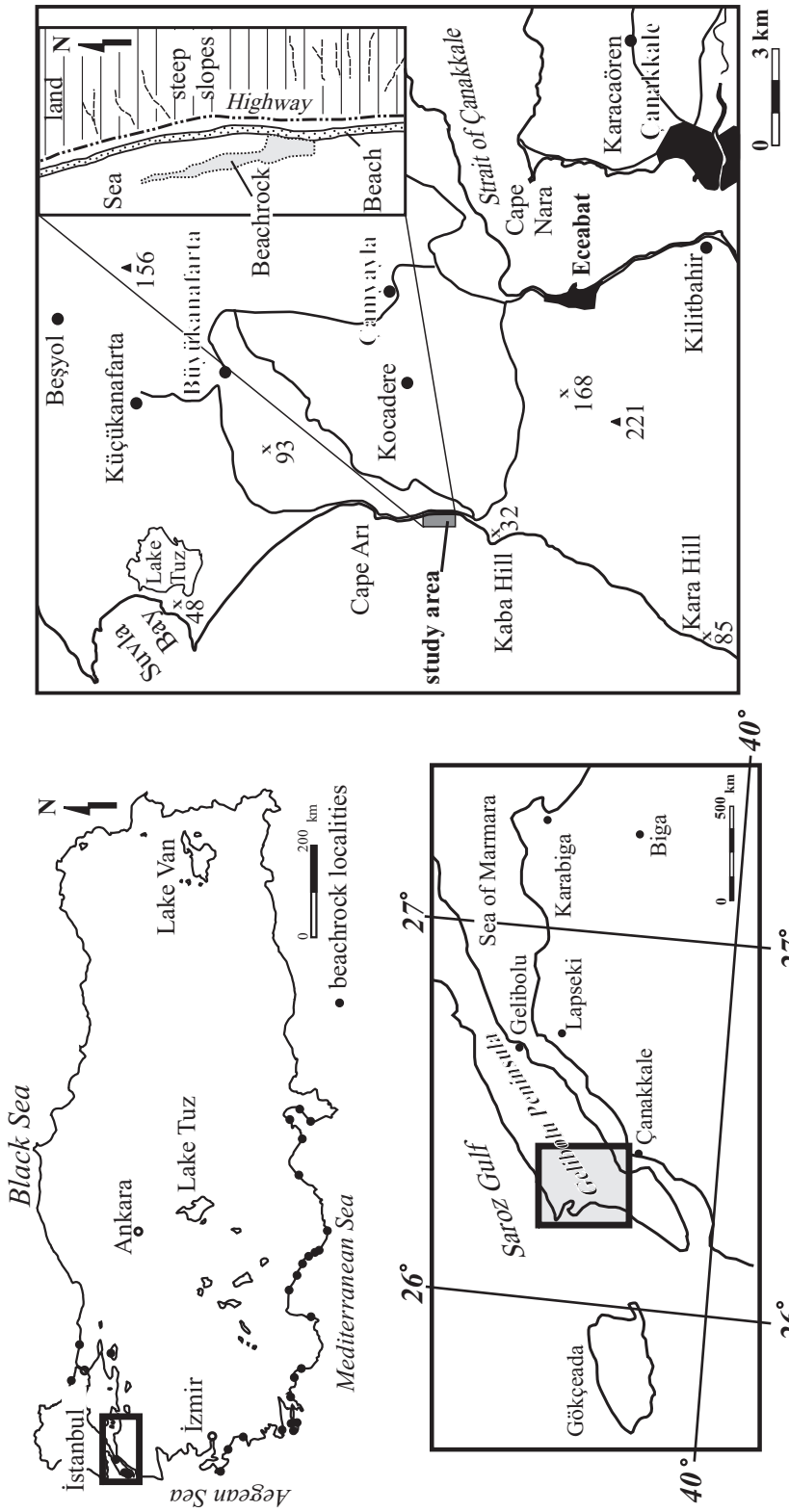

Figure 1. The distribution of beachrocks on Turkey's coastline and location of the study area.

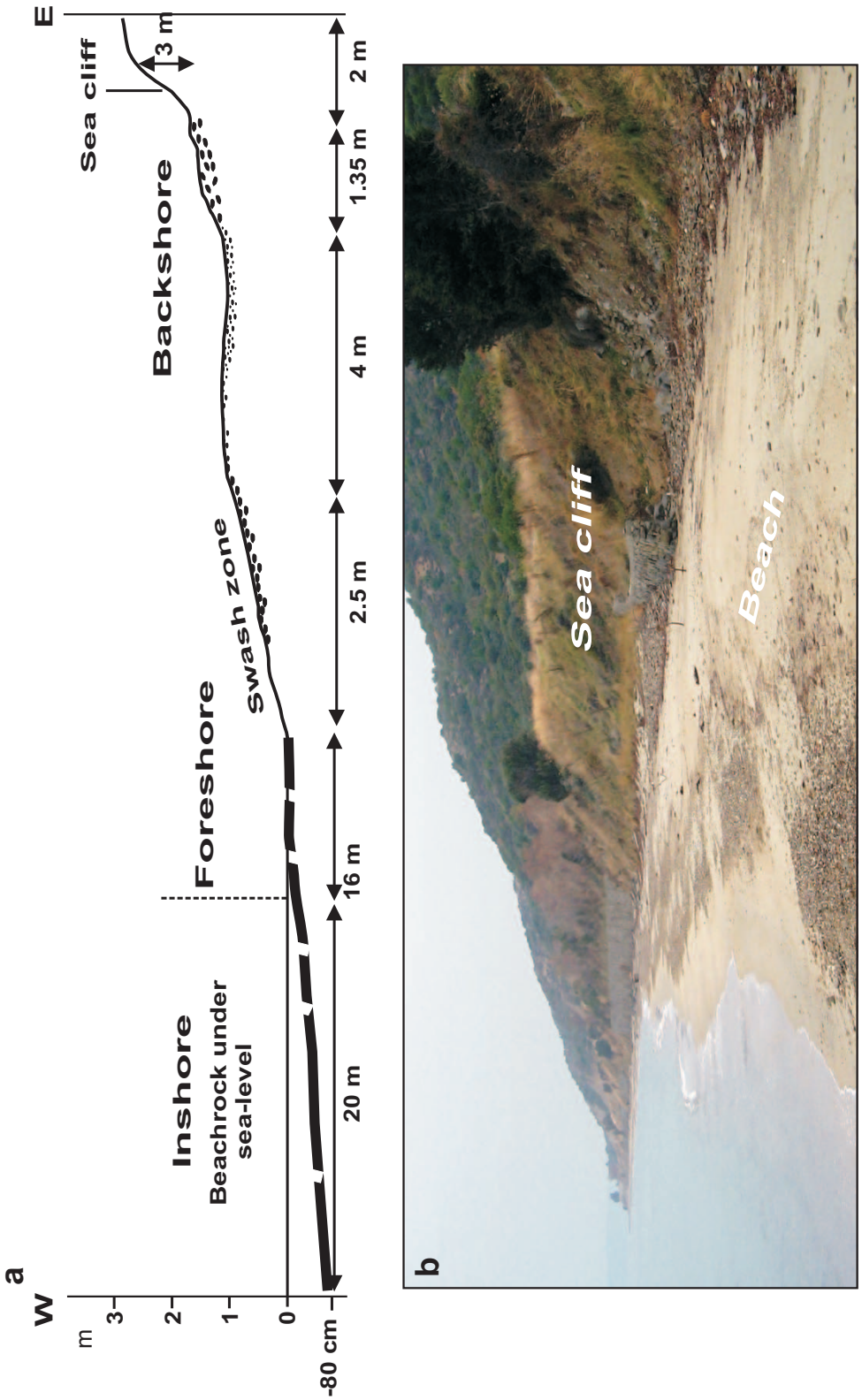

Figure 2. (a) Cross-section showing the extension of beachrock; (b) view of the adjacent beach in the study area.

cliff foot to the current shoreline, the beach slopes towards the sea at an angle of 3–5°. The seaward (wave swash zone) and landward (cliff foot) margins of the beach are characterized by gravels and boulders comprising quartz, sandstone, chert, gneiss and schist, limestone and serpentine. However, its middle part is almost entirely sandy with quartz grains, carbonate grains and, to a lesser extent, angular fragments of plagioclase and heavy minerals. On average the beach sands show a unimodal grain size frequency distribution and are well sorted and slightly skewed. Even though the dominant grain sizes range between 0.216 mm and 0.5 mm forming 60% to 90% of the overall composition, sands collected from the wave swash and the beach exhibit differences in size.

The wave swash zone is mainly represented by a dominant fraction ranging between 0.216 mm and 0.5 mm, less $CaCO_3$ content (10.2%) and slightly acidic pH (6.87). However, beach materials behind the wave swash are characterized by coarser sands, more $CaCO_3$ content (12%) and alkaline pH (8.12). Small amounts of fragmented residues of marine organisms such as *Ostrea edulis, Patella sp, Arca noae, Cardium edule, Ceritium vulgatum, Pecten maximus, Donax trunculus, Venus gallina* are sparsely scattered over the surface of the sandy beach.

Methods

Petrographic and Geochemical Analysis

Ten beachrock samples were collected for petrographic and geochemical analysis. Thin-section examinations were carried out by Olympus BX51 petrographic microscope. Several characteristics of beachrock loose beach sands (weighing 200–500), such as grain size distributions, total $CaCO_3$ content and pH were determined. $CaCO_3$ contents of the cements in eight beachrock samples were determined using a Scheibler calcimeter (Schlichting & Blume 1996) after dismissing clasts longer than 2 mm. pH measurements for the cement material were carried out using a WTW multi-parameter instrument based on the method of Grewelling & Peech (1960).

To determine total $CaCO_3$ content, eight powder samples of beachrocks were treated with dilute hydrochloric acid after coarse samples (>2 mm) were discarded. The grain size distributions of beach sands and beachrocks were analyzed by standard sieving techniques. For this purpose, a sub-sample weighing 200 g from each sample was dried in an incubator and then sieved through a set of standard sieves at $^1/_2$ ø intervals.

For the geochemical part of the work, ICP-AES analyses were applied in order to identify major and minor elements within the connective cement. For this purpose, each 1 g sample in dry weight was analyzed by ICP-AES by adding 10 ml of 1:1 HNO_3-HCL, mixing the slurry and covering with a vapour recovery device. The filtrated sample was analyzed by ICP-AES (Varian Axial Libery II Series ICP-AES) in the Central Laboratory of Çanakkale Onsekiz Mart University to determine major and trace elements in the beachrock cement.

Powder samples were also examined using EDS both to test accuracy of ICP-derived data and determine the quantity of Si. The crystal structures of minerals and cementation patterns were examined under JEOL JSM-5600 Scanning Electron Microscope (SEM) after coating the samples with a thin layer of gold by a Polaron SC 500 sputter coater.

Optically Stimulated Luminescence (OSL) Dating

To determine the age of the beachrock, five samples were taken for OSL dating, which relies upon the measurement of OSL signals. Thus, the last exposure to sunlight prior to deposition of sediments is accurately estimated. For OSL dating, samples YTS-01 and YTS-02 were taken from the top 5 cm (upper surface) and 10 cm (lateral surface) of beachrock beds, respectively. Three other samples (YTS-03, YTS-4, and YTS-05) were extracted from depths of 20–40 cm.

Samples were crushed and separated in the size range of 90–180 µm by wet sieving under subdued red light and first treated with HCL for the removal of carbonates, and then H_2O_2 for the organics. After HF treatment for etching the samples were treated with HCL once more prior to a distilled water wash. Six aliquots were prepared from quartz grains extracted from each sample and spread over stainless-steel discs using silicon spray. Then all aliquots were tested for feldspar contamination using infrared stimulation before OSL measurements. All measurements were undertaken using a Risø TL/OSL reader with blue (470 nm) light stimulation through U-340 filters (Bøtter-Jensen *et al*. 2000). For the environmental dose rate estimation, gamma dose rate was measured at site and spectral data were converted to dose rate used for the age calculation.

Equivalent Dose D_e and Growth Curves

The single-aliquot regenerative-dose (SAR) protocol was used to determine the equivalent dose absorbed by the samples during their burial time. The protocol based on a sequence of measurements using a single aliquot monitors and corrects for sensitivity changes between the measurement cycles (Murray & Wintle 2000). First the natural OSL signal (L_n) was measured following a preheat treatment of 260 °C, required for the removal of undesirable signals from the OSL curve. The sensitivity variation was monitored using the luminescence signal induced by a small test dose of 0.5 Gy (T_n, T_i). Then regenerative dose OSL signals (L_i) were measured in the following cycles at 125 °C for 40 s. L_n, L_i and T_n, T_i are derived from the OSL curve, taking the first 0.8s of the initial OSL signal, minus a background estimated from the last 4.0 seconds of the OSL signal. The luminescence response of the sample is corrected using the response of the test dose (L_n/T_n, corrected natural signal and L_i/T_i, corrected regenerative signal).

Dose Rate and OSL Ages

The gamma dose rates were measured on site and the beta dose rates were obtained from concentrations of the major radioactive isotopes of the uranium and thorium series and of potassium (Olley *et al.* 1996). The cosmic ray contribution to total dose rate was found to be in the range from 0.18 to 0.26 mGy/a depending on altitude, latitude and depth from the surface of each sample location (Prescott & Hutton 1988, 1994). The burial dose rates ranged from 1.25±0.03 to 1.30±0.03 mGy/a. The results of radiometric analysis and dose values obtained are summarized in Table 1 with errors due to statistical fluctuations in counting. The SAR ages of the samples taken from different profiles of the beachrock are also presented in Table 1 and the ages of the aliquots from each sample show good correlation. Figure 3 presents the growth curve for the beachrock quartz with the generative doses between 0 to 8 Gy defined by a mathematical function. The corrected natural OSL signal (L_n/T_n) and relevant equivalent dose D_e obtained by SAR are also presented.

Table 1. The results of radiometric analysis and dose values obtained.

Samples	SAR De (Gy)	Dose rate (Gy/ka)	n	Age (ka)
YTS-01	1.54±0.11	1.30±0.03	6	1.48±0.08
YTS-02	1.78±0.26	1.25±0.02	7	1.42±0.20
YTS-03	2.28±0.35	1.26±0.03	6	1.81±0.28
YTS-04	2.45±0.68	1.26±0.03	6	1.95±0.54
YTS-05	2.95±0.12	1.29±0.02	6	2.28±0.28

Results

Lithology

Beachrock beds comprising about 70–80-cm-thick lithified slabs of beach sands and gravels extend over 100 m in a north–south direction approximately parallel to the current shoreline and are characterized by tabular, highly-fractured, and friable beds that gently slope (about 3–5°) towards the sea (westwards). Although a limited part of the beds crop out at 50–60 cm above sea level (Figure 4a), the top of the beds can be followed down to about –1.00 m at their most seaward extent.

The petrographic composition of beachrock is almost entirely identical to that of the adjacent beach. Based on the textural characteristics of cemented clasts in descending order, two main lithofacies types can be identified: (1) poorly stratified and very poorly sorted conglomerate and (2) massive, well-stratified, moderately to well-sorted lithic arkose (Figure 4b).

Conglomerate consists on average of 15–20-cm-thick fragile slabs, comprising an assortment of several kinds of carbonate-cemented lithoclasts, such as sandstone, radiolarite, serpentine, limestone, gneiss and schist (Figure 4c) with small amounts of Eocene fossils such as *Pyrgo sp., Eofabiania sp., Discocyclina sp.* and A*ssilina sp*. The well-rounded pebbles have sizes ranging between 5 cm to over 10 cm. On the basis of calcimetric measurements, the rock has a total carbonate cement of 59.08 %. Sieving analysis showed that 70% of the cemented material was in the size fraction of 1–2 mm, implying a predominance of coarse sand. Morphologically, the upper surfaces of the beds are characterized by very shallow depressions of circular shape as a result of erosion, biological processes and solution. The broken and abraded parts of the beachrock most commonly occur along joint systems and the uppermost parts of the beds are green to brown in colour due to the presence of algae, such as *Chlorophyta sp., Closterium sp., Cocconeis sp., Cystoseira sp., Gyrosigma sp., Heliozoa sp., Licmophora sp., Navicula sp., Oscillatoria sp., Phormidium sp., Pinnularia sp, Rivularia sp., Stephanodiscus sp., Surirella sp. and Tabellaria sp.* Marine organisms such as *Semibalanus balanoides and*

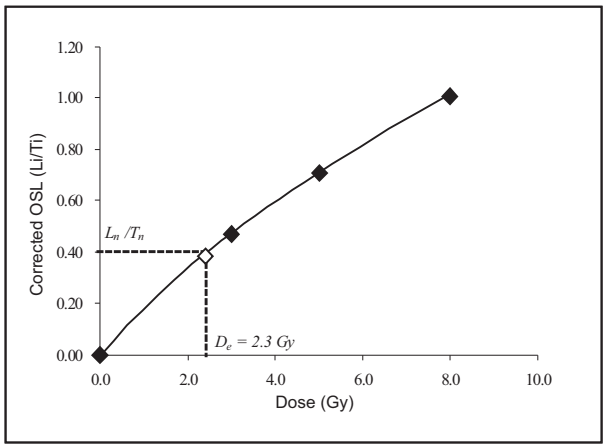

Figure 3. Growth curves of a quartz from beachrock for a dose range between 0 and 8 Gy. Quartz minerals collected from various strata of beachrock show almost identical growth curves, corrected for sensitivity changes by the subsequent OSL test dose response (L_i/T_i). D_e is corresponding to the corrected natural OSL signal (L_n/T_n).

Patella sp. feed on this algae cover mostly on the upper surface of the ledges. The pH of the cement material is alkaline (8.83).

The underlying lithic arkose is made up of coarse sands and very small gravels ranging in size between 0.5 cm and a few cm (Figure 4d). Based on Folk's (1970) classification, it is lithic arkose in composition and forms the main body of the beachrock beds with an average thickness of 60 cm. The polycrystalline quartz grains, feldspar grains, biotite and opaque minerals as main constituents were identified in thin sections and crystal sizes range in general from 0.1 mm to more than 1 mm. From sieving analysis, it was found that approximately 56% of the grains range in size between 1.00 and 2.00 mm. Subsequent grain sizes of 0.5–1.00 mm form about 22% of the bulk rock volume. $\sum CaCO_3$ and pH are 36% and 8.75, respectively.

The overall assessment of the mineral composition of beachrocks under thin-section images indicated the presence of several types of mineral fragments in various amounts (Figure 4e, f). Feldspar is found at the total average amount of 10–15%. The predominant form of mineral form is plagioclase characterized by polysynthetic twins. In some cases, sericite and epidote crystals were visible on surfaces of the plagioclase as common alteration minerals. Opaque minerals were either angular or spherical shaped grains with crystal sizes ranging between 0.2 mm and 0.5 mm. Mica (mainly biotite), found within the small fragments of schist and gneiss, has a proportion of 3–5%. Many of the siliciclasts and lithoclasts are moderately or poorly rounded, implying either that they have not been worn much by wave activity or that their source-area was close to the beach where the beachrock cementation has taken place.

Elemental Composition of Sea Water and Beachrock Cement

In order to make a simple comparison between elemental composition of sea water and powder samples of beachrock cements, ICP-AES analysis were carried out. Regarding the sea water composition, the data reveal that the predominant ion is Na (85%) with a concentration of 5675 ppm, followed by Mg, K and Ca with concentrations of 371 ppm (5.5%), 402 ppm (6%) and 244 ppm (3.6%), respectively. The rest of the components except Sr (4.94 ppm) and B (3.44 ppm) are present in amounts less than 1 ppm, having only a very small fraction of 0.12 % within the overall composition (Figure 5a).

The results of ICP-AES analysis exhibit rather different elemental compositions for beachrock cements. From the analysis, Ca (Figure 5a) was found to be the main constituent forming 70.3% of the total composition. However, its total amount showed a significant difference between conglomeratic beachrock (56257 ppm or 75.9%) and underlying lithic arkose (36337 ppm or 64.7%). Al and Fe as the other important constituents constituted 11% and 9.65% of overall composition, respectively. When compared with high Ca content, Na, Mg and K were found to be very scant forming only approximately 8.2% of the total.

EDS analysis which was employed upon five representative samples to determine Si content and test the accuracy of ICP-derived data showed that Si and Ca, (Figure 5b) form the highest components with average proportions of 36.2% and 32.68%, respectively. Al and Fe, however, occupy about 16% of the total elemental composition. The other elements, i.e. Na, Mg, K, Cr, Mn, Cu, Zn, Ba and Pb together formed 15% of the total composition.

Micromorphological Features

After analytical determination of the average amounts of $CaCO_3$, and major and trace elements, cement micromorphologies or crystal shapes within the studied

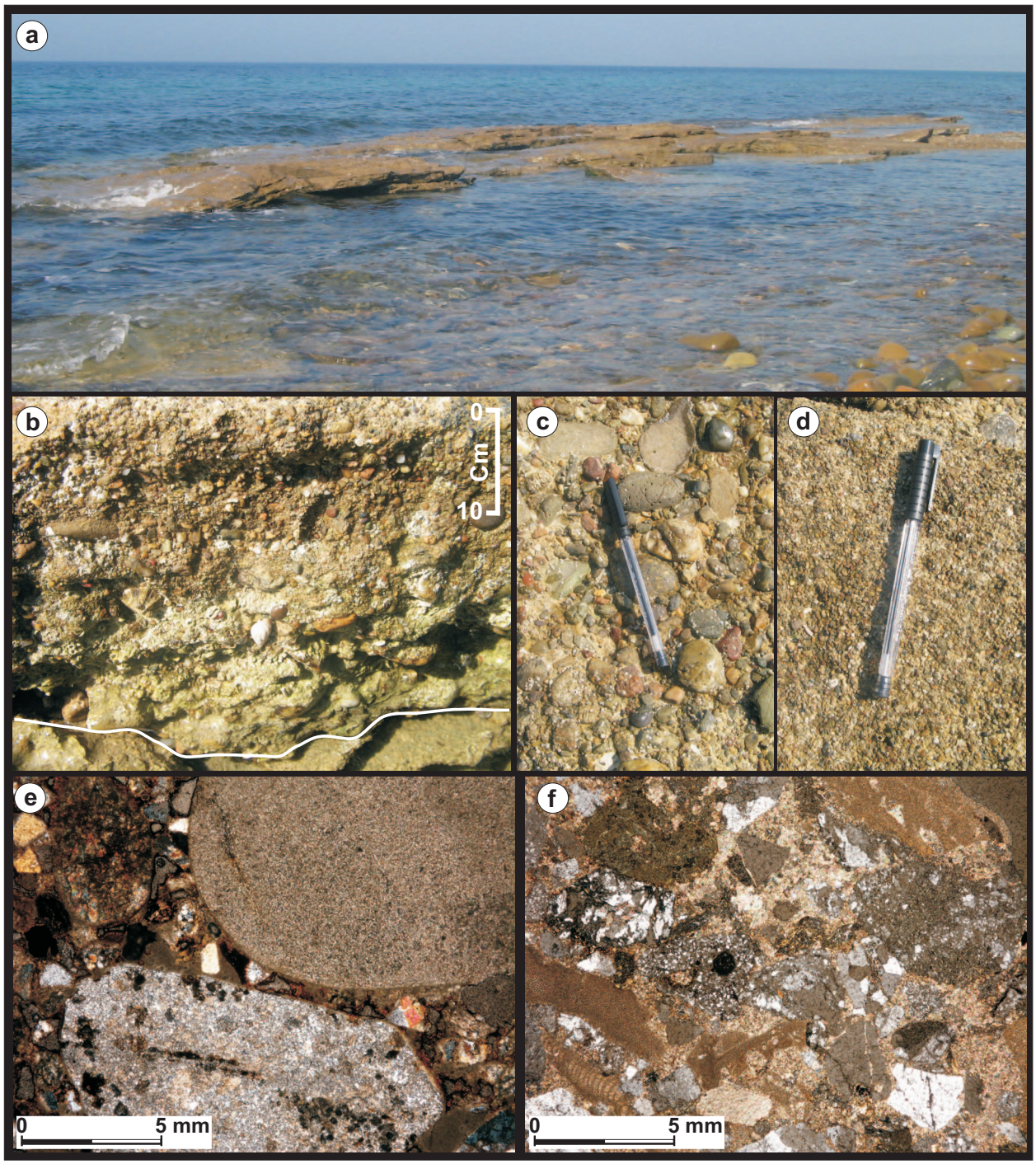

Figure 4. (a) Beachrock outcrops studied; (b) a close view of the beachrock sequence [white line separates the conglomerate and lithic arkose]; (c–d) closer views of conglomerate and lithic arkose, respectively; (e–f) thin section images of poorly stratified and very poorly sorted conglomerate and massive, well-stratified, moderately to well sorted lithic arkose, respectively.

beachrocks were defined to shed light on the nature of diagenetic processes. To this end, EDS results and SEM images were used. From EDS analysis, high-Mg calcite was found to be the predominant cement material of the beachrock beds.

Four main stages of cementation were determined that include the following morphologies: (1) micritic coatings, (2) cryptocrystalline pore-filling cement, (3) meniscus cement, and (4) microbial cement. The cement micromorphology within the beachrock cements is explained below on the basis of SEM image interpretations.

On the uppermost surface of beachrock, some evidence of endolithic activity within the studied beachrocks suggests, at least in part, the presence of biological control on cementation. Microbial cement occurrence was determined on the upper conglomeratic beachrock layers where colonization by cyanobacteria and molluscan gastropods is a common feature (Figure 6a). This cement is characterized by randomly distributed needle-fibre growths, fungal filaments and associated traces of microorganism borings.

The filaments showing chaotic occurrences on rock barnacles are more than 100 µm in length and curved in shape (Figure 6b). Small calcite crystals are also observed on the surface of the filaments, some of which appeared as calcified structures.

The microbial cement is mainly characterized by needle-fibre cement, which is mainly composed of 10–50 µm long monocrystals (Figure 6c). The needles vary in thickness ranging between 5 and 10 µm and calcite precipitations as overgrowths on and between needles are common. Some traces of microorganism scratches are present within the needles (Figure 6d).

Conglomerate is observed with three types of cements predominant within the cement micromorphology, namely (1) micritic coatings, (2) cryptocrystalline pore-filling cement and (3) meniscus cement. The rock is composed mainly of poorly rounded or angular siliciclastic grains ranging in size between 500 µm and 3.5 mm (Figure 7a). Each siliciclastic grain seems to be covered by thin (between 5–10 µm in thickness), double microcrystalline Mg-calcite coatings. This cement is rough in morphology and, in many places, composed mainly of blade-shaped clumps of Mg-calcite crystals. Closer examination of the crystals shows the presence of scalenohedral terminations; 5–10 µm in length and having maximum 5 µm widths. Although in some places they display irregular scattering on mineral surfaces, mineral contacts are characterized by very dense and amalgamated crystals (Figure 7b). Radial aggregates with diameters ranging between 10 µm (0.01 mm) and 30 µm (0.03 mm) are well developed on micritic envelopes (Figure 7c).

Overgrowth of scalenohedral Mg-calcite crystals within the pores lead to a decrease in porosity, which is largely associated with widespread precipitation of micritic pore-filling cement on micritic envelopes. This type of cementation is mainly marked by plasters over and between the broken or angular-shaped siliciclastic grains with sizes lesser than 500 µm (Figure 7d). The cement material is composed mainly of equigranular (average size: 10 µm) prismatic Mg-calcite crystals.

Meniscus of carbonate precipitates which could be seen as bridges (average thick: 150–200 µm) among angular siliciclastic grains is observed within some SEM images (Figure 7e, f). This is a mixture of carbonate precipitates with micrometric-scale siliciclasts. Closer view of the cement micromorphology shows that these menisci have developed on thin micritic coatings.

Lithic arkose had similar characteristics (i.e. fabrics and cement micromorphologies) to that of the overlying conglomerate, except for significant reduction in grain sizes. Cementation, in general, seems to be well developed along broken or flat parts of the grains. Angular and very poorly rounded grains within the size range of 500 µm and 1 mm forms the cementation, as revealed by the SEM images. The contact between microcrystalline Mg-calcite crystal coatings (Figure 8a) and fine-grained materials was difficult to observe due to the densely developed micritic pore-filling cement with pseudo-peloids (Figure 8b, c). Meniscus-style cement of rare occurrence is represented by very thin bridges (about 500 µm or less) between the fine grains (Figure 8d).

Discussion

Pre-cementation Environment

At the Arıburnu beach, beachrocks extend nearly parallel to the present shoreline and have similar lithological characteristics to the present beach. Their most conspicuous morphologic feature is that a very limited part of the beachrock (40–60 cm in vertical section) is exposed at the present shoreline. However, the subhorizontal beds were followed down to –1 m (20 m offshore from the present shoreline).

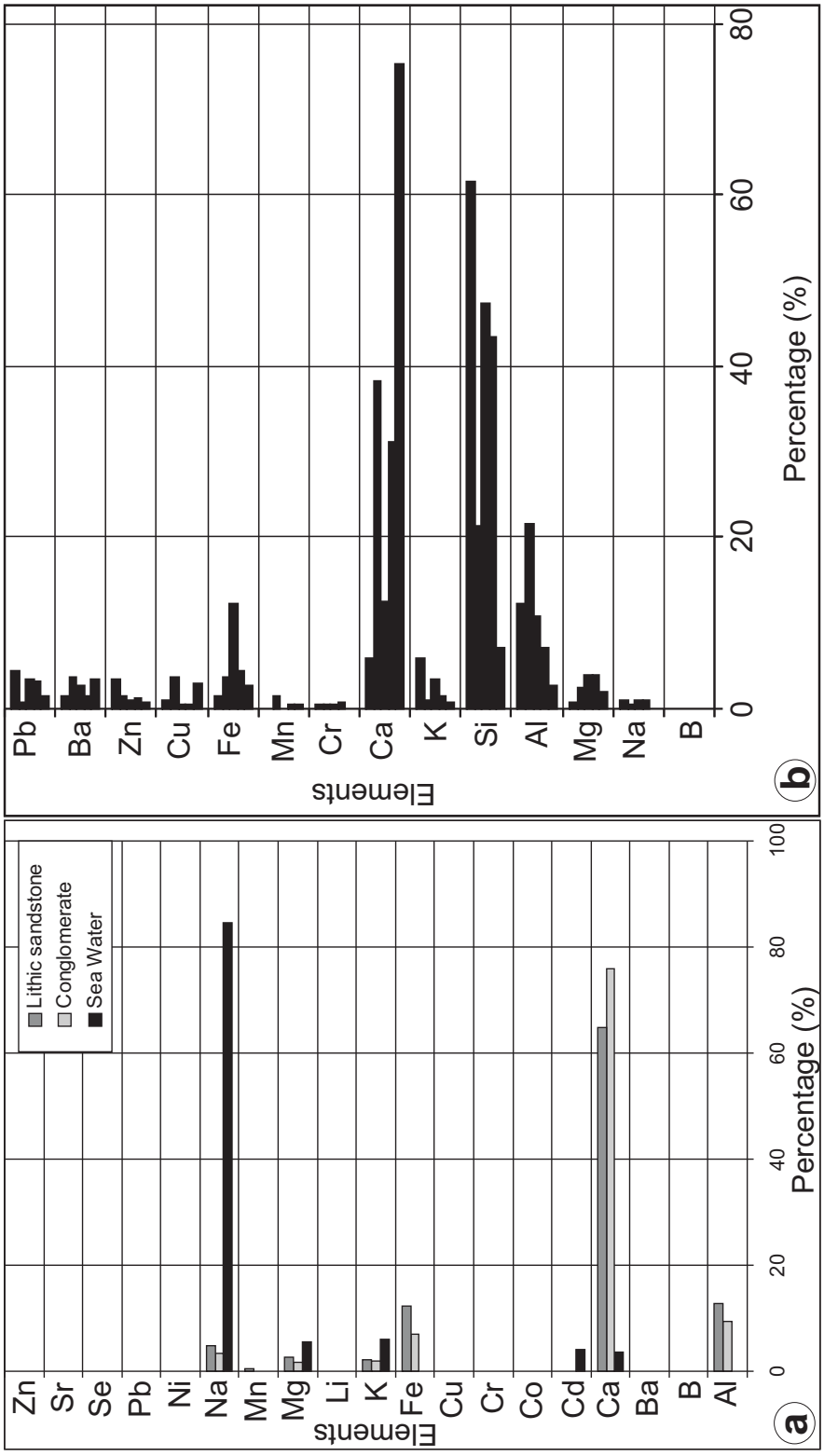

Figure 5. (a) ICP-AES analysis results derived from beachrock cements and sea water; (b) EDS results from powder samples of beachrock cement.

Figure 6. Microbial cement occurrences on the upper conglomeratic beachrock layers. **(a)** Fungal filaments under rock barnacles; **(b)** detail views of (a) calcified filaments. Arrows display growth of calcite on the curved filaments; **(c)** needle-fibre cement characterized by chaotically dense patches: arrows display calcite precipitations on flat crystal surfaces; **(d)** traces of microorganism boring marks within the needles as shown by arrow.

Sieving analyses, which are in good agreement with the results of thin section analysis, indicate that most of the cemented material (60–70%) is composed of grains within the size class between 1 and 2 mm. The present loose beach materials are, however, made up of finer grains ranging in size between 0.216 mm and 0.5 (60–70%) with the exception of storm berm deposits on the swash zone, likely implying that the pre-cementation environment might have been dominated by higher energy conditions. In addition, unconsolidated beach materials had lesser amounts of $CaCO_3$ (10–12%) and a lower degree of pH (6.87–8.12) compared with those measured from the upper and the lower sections of beachrock beds ($\sum CaCO_3$: 59.08–36%; pH: 8.83–8.75, respectively). These results

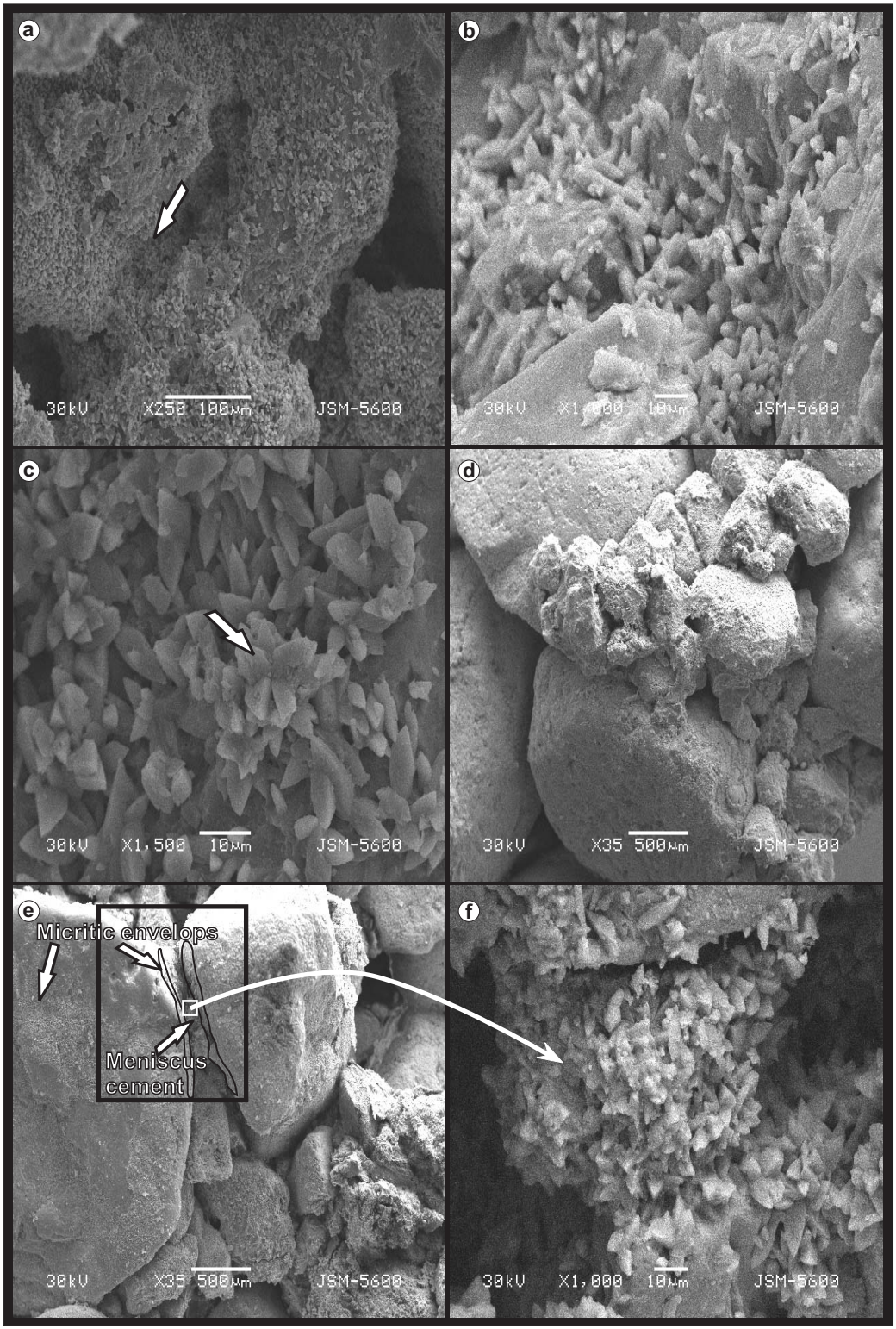

Figure 7. SEM images displaying various micromorphologies of cement within the conglomeratic beachrock. **(a)** Microcrystalline micritic coatings on siliciclastic grains; **(b)** enlargement of (a); **(c)** radial aggregates of high-Mg calcite crystals with scalenohedral terminations; **(d)** cryptocrystalline pore-filling cement; **(e)** menisci bridging between the angular siliciclastic grains; **(f)** close up view of (e).

may imply that production and following precipitation of carbonate cement occurred in relatively different conditions than those of today.

Another significant feature of the beachrocks is that they comprise a maximum 80 cm thickness of indurated beds. When compared with other examples of beachrock from Turkey's coasts, such as those with 4 m thickness that occur on the coastline between Alanya and Gazipaşa (Bener 1974; Kelletat 2006), the Arıburnu beachrocks reflected typical conditions for cementation on microtidal environments, which vary between 0.20 m and 0.60 m in thickness in the eastern Mediterranean (Kelletat 2006). For the Arıburnu coast, several field observations show that the tidal range was between 30 and 40 cm. At high tide periods, most of the beds with the exception of upper surfaces of the beds (10–20 cm) became submerged. Thus, it can be stated that the studied beachrocks seem to be found at or near the present environment of formation.

However, the presence of submerged beachrock beds at –1 m offshore level poses a problem that needs to be explained. This condition is actually a well-known significant problem for beachrock investigations, because explanations are widely restricted within the exposed formations (Vousdoukas *et al*. 2007). However, a total vertical difference of 160 cm between the most seaward (submerged at –1 m) and landward (exposed at maximum 60 cm asl) edges of the beds simply revealed sea-level variations and, more importantly, higher tidal range conditions for the time when beachrock cementation took place.

The Genesis of Beachrock and Cementation History

Both elemental composition and SEM examinations of the analyzed samples simply reflected the genesis of beachrock cementation in the Arıburnu beach. EDS analysis reveals that carbonate cements are commonly high-Mg calcite like the most common cement of many recent beachrocks (Ginsburg 1953; Alexanderson 1969; Taylor & Illing 1969; El-Sayed 1988; Gischler & Lomando 1997). It is likely that precipitation of carbonate cement was facilitated by the common presence of angular siliciclastic and carbonate grains, among which porosity was quite suitable for free circulation of water (Moore 1989).

Our results reveal that carbonate precipitation as suggestive of different diagenetic processes was associated with three main processes: (1) supersaturation of $CaCO_3$ by evaporation of sea water, (2) such as mixing of marine and meteoric water fluxes, and (3) biological cementation. From SEM examinations, four main morphologies were identified in Mg-calcite and aragonite cements: (1) micritic coatings, (2) cryptocrystalline pore-filling cement, (3) meniscus cement and (4) microbial cement. The direct precipitation because of the evaporation of sea water was the most significant process as evidenced by the widespread occurrence of high-Magnesian calcite with a micritic texture at various morphologies, such as thin coatings and, more importantly, cryptocrystalline pore-fillings.

Regarding the diagenetic history, the commencement of cement precipitation started with the formation of micritic coatings both on the surface and, in some places, on the broken edges of the angular grains. These coatings which formed the most common cement micromorphology suggest rapid supersaturation of pore waters (Scoffin 1987) as an explanation for the initial diagenesis of beachrocks (Beier 1985; Neumeier 1999; Vieira & De Ros 2007). The wide growth of radial aggregates as prismatic crystals or pseudo-peloids on these envelops reveals the continuation of micritic cement accumulation under supersaturation of $CaCO_3$ by evaporation of sea water. The development of these radiating crystals, which occurred preferentially on the surfaces of siliciclastic grains, constituted the subsequent diagenetic event as recently evidenced by Vieira & De Ros (2007).

The initial precipitation of micritic coatings and radial aggregates is followed by the formation of cryptocrystalline pore-fillings, which is the most extensive cement in abundance in the studied beachrocks. The presence of this cement, which has been defined as a common feature of well-cemented beachrocks (Gavish & Friedman 1969; Webb *et al*. 1999), explains the ongoing rapid cementation under active marine phreatic zone (Vieira & De Ros 2007). Nevertheless, no microbial contribution to the precipitation of these cements was detected under SEM images, although proposed by previous publications such as Kneale & Viles (2000) and Calvet *et al*. (2003).

Meniscus bridges as an indicator for another diagenetic process took place in the studied samples. This cement is found in both layers of the beachrock, namely in conglomerate and lithic arkose, implying infiltration from carbonate-rich meteoric waters (Friedman 1964; Folk 1974; Scoffin & Studdart 1983; Spurgeon *et al*. 2003; Rey *et al*. 2004) filling the interparticle porosity (Vieira &

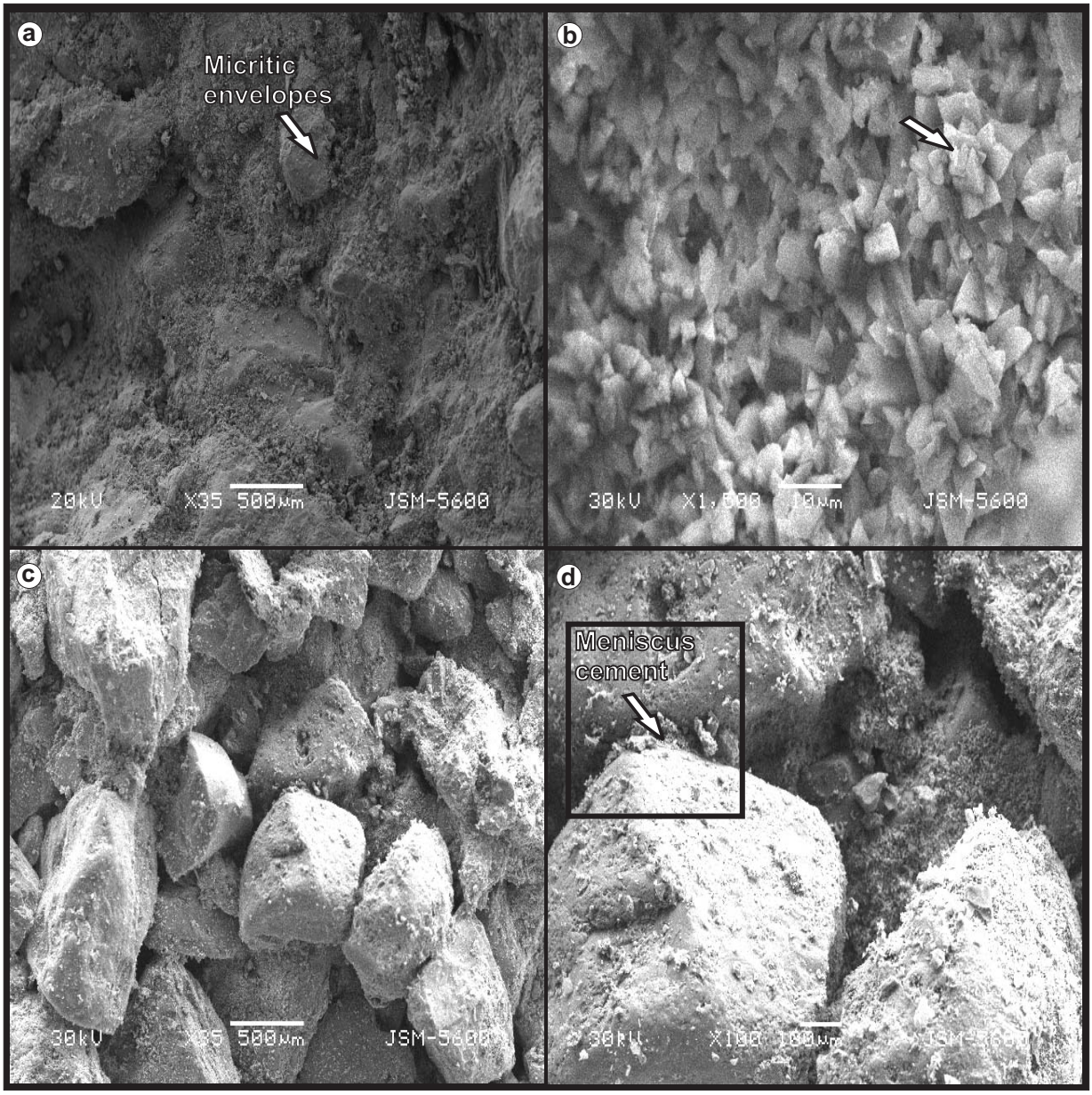

Figure 8. SEM images displaying micromorphologies of cement within the lithic arkose. **(a)** Micritic envelops on siliciclastic grains; **(b)** enlargement of (a); **(c)** cryptocrystalline pore-filling cement; **(d)** meniscus cement.

De Ros 2007). Its co-existence with the above-mentioned marine cements was not an unusual condition in beachrocks (Hanor 1978) with the exception of those in the Mediterranean where this mechanism has been rarely determined (Vousdoukas *et al*. 2007). Actually, mixing of marine and meteoric water fluxes (Schmalz 1971; Moore 1973) enables suitable conditions for precipitation of such cements through, for example, causing changes in Ph and increasing the concentration of dissolved carbonates (Rey *et al*. 2004). Thus, the precipitation of meniscus cement indicates that the active marine phreatic zone conditions were probably contributed to by meteoric water fluxes.

The last diagenetic cement was of biological origin in the Arıburnu beachrocks. This kind of cement within the studied samples was found on the uppermost surface of conglomeratic beds and consists of needle-fibre growths

and curve-shaped fungal filaments. Similar examples of needle-fibre cement have been described by several authors (Jones & Kahle 1993; Verrecchia & Verrecchia 1994; Webb *et al.* 1999; Khadkikar & Rajshekkar 2003) and are interpreted to provide evidence of biologically-mediated precipitation of beachrock cement under marine phreatic conditions.

Age of Beachrock

OSL ages obtained from quartz samples yield minimum and maximum ages of 1.42±0.20 ka and 2.28±0.28 ka, respectively, indicating a time interval of 0.8 ka during the cementation period. The age values increase upwards in vertical section. Similar estimated ages were obtained on the Galicia coast of northwest Spain by Rey *et al.* (2004) and younger ones in Belize by Gischler & Lomando (1997). These values yield rather younger ages compared to those of the eastern Mediterranean beachrocks, which were mostly cemented between 4000 and 2000 BP (Kelletat 2006). However, the obtained results reflect the ages for exposed beachrock at the upper intertidal zone. On the assumption that onshore buried parts of the beachrock beds mostly represent younger stages of cementation (see detailed discussion by Vousdoukas *et al.* 2007), future studies on dating the submerged parts of the beachrock ledges at their most seaward extent could be expected to yield older ages. Thus, it can be suggested that sea level was almost at the same position during the last 2000 years when the induration of exposed beachrock materials on the upper beach were occurring. In other words, sea level might have continually risen up to its current position following the cementation of submerged beachrock of unknown age.

Conclusions

From the presented petrographic and geochemical analysis, we derived the following preliminary results:

(1) The Arıburnu beachrocks are composed of highly-fractured and friable beds. Petrographically, two lithofacies are identified: weakly stratified, very poorly sorted conglomerate and massive, well-stratified, moderately to well-sorted lithic arkose. The beachrock beds contain poorly rounded siliciclasts and lithoclasts, which likely indicates that these grains and gravels have not been worn much by wave activity. Various mineral fragments such as polycrystalline quartz, feldspar, biotite and heavy minerals occur in various amounts.

(2) The beachrock cements appeared to be enriched with $CaCO_3$ that decreases from 59.08% to 36% in depth. Si and Ca forms the main constituent of elemental composition with average rates of 36.2% and 32.68%, respectively, which were followed by Al and Fe having forming 16% of the total composition. Based on ICP-AES and EDS data, Mg was found at average amounts of 2.11% and 2.63 %, respectively. EDS analysis also reveals that carbonate cements in the studied beachrocks are commonly high-Mg calcite like the most common cement of many recent intertidal beachrocks in the world.

(3) Mg-calcite cements were found to have occurred with four main morphologies, namely: (i) micritic coatings, (ii) cryptocrystalline pore-filling cement, (iii) meniscus cement, and (iv) microbial cement. Cementation history may have begun with precipitation of micritic coatings as the early cements on the surface of grains and is followed by pore-filling cement co-existed with meniscus bridges. Apart from rarely observed meniscus structures that were suggestive of the presence of meteoric environment conditions at some successive phases of cementation history, the whole cement types suggest the intertidal or marine phreatic zone.

In conclusion, the present study explains the main factors co-acting during the diagenetic process and demonstrates that the studied cemented material was truly an intertidal beachrock in the strict sense and does not exhibit any strong evidence for cementation in another environment such as the supratidal zone.

The OSL-SAR protocol was successfully applied to quartz grains extracted from beachrock deposits and encourages future relevant studies in this area. It is remarkable that the growth curves are presented by the same exponential function for all samples provided from each profile. The luminescence ages are lower for the samples taken close to the edge of the beachrock beds. These values are relatively higher for the samples taken from inner parts. Finally for further investigation, the OSL-SAR technique has great potential for obtaining an accurate chronology for better understanding beachrock occurrences in this area.

Acknowledgements

We would like to thank Muhammed Z. Öztürk and Gökhan Altan for assisting the fieldwork and Rıza Akgül for microscopic examination of the samples. Murat Türkeş is thanked for proofreading. We extend our thanks to Mahmut Coşkun and Akın Çayır for preparing the powder samples of beachrock cement for ICP-AES analysis. Murat Manaz is thanked for support in sample preparation for OSL analysis. The authors appreciate the constructive comments on the manuscript by journal reviewers (Jasper Knight and an anonymous reviewer) whose comments greatly improved the paper. Our thanks also go to John D. Piper for his invaluable help in the English editing of the final text.

References

ALEXANDERSON, T. 1969. Recent littoral and sublittoral high-Mg calcite lithification in the Mediterranean. *Sedimentology* **12**, 47–61.

ALEXANDERSON, T. 1972. Mediterranean beachrock cementation: marine precipitation of Mg-calcite. *In:* STANLEY, D.J. (ed), *The Mediterranean Sea*. Dowden, Hutchinson and Ross, 203–223.

AVŞARCAN, B. 1997. Theories on beachrock formation and some characteristics of beachrocks on Turkey's coasts. *Geographical Journal of İstanbul University* **5**, 259–282 [in Turkish with English abstract].

BEIER, J.A. 1985. Diagenesis of Quaternary Bahamian beachrock: petrographic and isotopic evidence. *Journal of Sedimentary Petrology* **55**, 755–761.

BENER, M. 1974. *Beachrock Formation on the Coastal Part of Antalya-Gazipaşa*. İstanbul University Institute of Geography Publications no. **75** [in Turkish].

BRICKER, O.P. 1971. Introduction: beachrock and intertidal cement. *In:* BRICKER, O.P. (ed), *Carbonate Cements.* John Hopkins Press, Baltimore, M.D, 1–3.

BØTTER-JENSEN, L., BULUR, E., DULLER, G.A.T., MURRAY, A.S. 2000. Advances in luminescence instrument systems. *Radiation Measurements* **32**, 523–528.

CALVET, F., CABRERA, M.C., CARRACEDO, J.C., MANGAS, J., PEREZ-TORRADO, F.J., RECIO, C. & TRAVE, A. 2003. Beachrocks from the island of La Palma (Canary Islands, Spain). *Marine Geology* **197**, 75–93.

DMİ (Devlet Meteoroloji İşleri Genel Müdürlüğü) *Monthly Precipitation Data Recorded at Gökçeada Meteorological Station During the Period of 1972–2003* [in Turkish].

EL-SAYED, M.K.H. 1988. Beachrock cementation in Alexandria, Egypt. *Marine Geology* **80**, 29–35.

EROL, O. 1972. Beachrock formations on the Gelibolu Peninsula coast. *Geographical Journal of Ankara University* **3–4**, 1–2 [in Turkish].

EROL, O. 1983. Historical changes on the coastline of Turkey. *In:* BIRD, C.F.E. & FABBRI, P. (eds), *Coastal Problems in the Mediterranean Sea*, 95–108.

ERTEK, T.A. 2001. Neotectonic movements and beachrock formation on the coasts between Sahilköy and Şile. *Quaternary Workshop of Turkey, İstanbul Technical University, Proceedings*, 24–31 [in Turkish].

ERTEK, T.A. & ERGINAL, A.E. 2003. Physical properties of beachrocks on the coasts of Gelibolu Peninsula and their contribution to the Quaternary sea level changes. *Turkish Journal of Marine Science* **9**, 31–49.

FOLK, R.L. 1974. The natural history of crystalline calcium carbonate: effect of magnesium content and salinity. *Journal of Sedimentary Petrology* **44**, 40–53.

FOLK, R.L., ANDREWS, P.B. & LEWIS, D.W. 1970. Detrital sedimentary rock classification and nomenclature for use in New Zealand. *New Zealand Journal of Geology and Geophysics* **13**, p. 955.

FRIEDMAN, G.M. 1964. Early diagenesis and lithification in carbonate sediments. *Journal of Sedimentary Petrology* **34**, 777–813.

FRIEDMAN, G.M. & GAVISH, E. 1971. Mediterrenean and Red Sea (Gulf of Aqaba) beachrocks. *In:* BRICKER, O.P. (ed), *Carbonate Cements*. The Johns Hopkins Press, Baltimore, M.O, 13–16.

GAVISH, E. & FRIEDMAN, G.M. 1969. Progressive diagenesis in Quaternary to Late Tertiary carbonate sediments: sequence and time scale. *Journal of Sedimentary Petrology* **39**, 980–1006.

GINSBURG, R.N. 1953. Beachrock in South Florida. *Journal of Sedimentary Petrology* **23**, 85–92.

GISCHLER, E. & LOMANDO, A.J. 1997. Holocene cemented beach deposits in Belize. *Sedimentary Geology* **110**, 277–297.

GOUDIE, A. 1966. A preliminary examination of the beach conglomerates of Arsuz, South Turkey. *Geographical Articles* **6**, 6–9.

GREWELLING, T. & PEECH, M. 1960. *Chemical Soil Test*. Cornell University Agricultural Experiment Station Bulletin no. **960**.

GUILCHER, A. 1965. *Précis d'Hydrologie. Marine et Continentale*. Masson, Paris, New-York, Barcelone, Milane.

HANOR, J.S. 1978. Precipitation of beachrock cements: mixing of marine and meteoric waters vs. CO_2 degassing. *Journal of Sedimentary Petrology* **48**, 489–501.

HOLAIL, H & RASHED, M. 1992. Stable isotopic composition of carbonate-cemented recent beachrock along the Mediterranean and Red Sea coasts of Egypt. *Marine Geology* **106**, 141–148.

JONES, B. & KAHLE, C.F. 1993. Morphology, relationship, and origin of fiber and dendrite calcite crystals. *Journal of Sedimentary Research* **63**, 1018–1031.

KELLETAT, D. 2006. Beachrock as a sea-level indicator? Remarks from a geomorphological point of view. *Journal of Coastal Research* **22**, 1555–1564.

KHADKIKAR, A.S. & RAJSHEKKAR, C. 2003. Microbial cements in Holocene beachrocks of South Andaman Islands, Bay of Bengal. *Current Science* **84**, 933–936.

KNEALE, D. & VILES, H.A. 2000. Beach cement: incipient $CaCO_3$ – cemented beachrock development in the upper intertidal zone, North Uist, Scotland. *Sedimentary Geology* **132**, 165–170.

KRUMBEIN, W.E. 1979. Photolithotropic and chemoorganotrophic activity of bacteria and algae as related to beachrock formation and degradation (Gulf of Aqaba, Sinai). *Geomicrobiology Journal* **1**, 156–202.

MEYERS, J.H. 1987. Marine vadose beachrock cementation by cryptocristalline magnesian calcite-Maui, Hawaii. *Journal of Sedimentary Petrology* **57**, 755–761.

MOORE, C.H. 1973. Intertidal carbonate cementation, Grand Cayman, West Indies. *Journal of Sedimentary Petrology* **43**, 591–602.

MOORE, C.H. 1989. *Carbonate Genesis and Porosity*. Elsevier, Amsterdam.

MOORE, C.H.JR. & BILLINGS, G.K. 1971. Preliminary model of beachrock cementation, Grand Cayman Island, B.W.I. *In:* BRICKER, O.P (ed), *Carbonate Cements*. John Hopkins Press, Baltimore, M.D, 40–43.

MURRAY, A.S. & WINTLE, A.G. 2000. Luminescence dating of quartz using an improved single-aliquot regenerative-dose protocol. *Radiation Measurements* **32**, 57–73.

NEUMEIER, U. 1998. Le rôle de l'activité microbienne dans la cimentation précoce des beachrocks (sédiments intertidaux). *Terra Environ* **12**, 1–183.

NEUMEIER, U. 1999. Experimental modelling of beachrock cementation under microbial influence. *Sedimentary Geology* **126**, 35–46.

OLLEY, J.M, MURRAY, A.S., ROBERT, R.G. 1996. The effects of disequilibria in the uranium and thorium decay chain on burial dose rates in fluvial sediments. *Quaternary Science Reviews* **15**, 751–760.

PRESCOTT, J.R. & HUTTON, J.T. 1988. Cosmic ray and gamma ray dosimetry for TL and ESR. *Nuclear Tracks Radiation Measurements* **14**, 223–227.

PRESCOTT, J.R. & HUTTON, J.T. 1994. Cosmic ray contribution to dose rates for luminescence and ESR dating: large depths and long-term time variations. *Radiation Measurements* **23**, 497–500.

REY, D., RUBIO, B., BERNABEU, A.M. & VILAS, F. 2004. Formation, exposure, and evolution of a high-latitude beachrock in the intertidal zone of the Corrubedo complex (Ria de Arousa, Galicia, NW Spain). *Sedimentary Geology* **169**, 93–105.

SCHLICHTING, E. & BLUME, E. 1996. *Bodenkundliches Practicum*. Verlag paul Parey, Hamburg und Berlin.

SCHMALZ, R.F. 1971. Formation of beachrock at Eniwetok Atoll. *In:* BRICKER, O.P. (ed), *Carbonate Cements.* Johns Hopkins Press, Baltimore, MD, 17–24.

SCOFFIN, T.P. 1970. A conglomeratic beachrock in Bimini, Bahamas. *Journal of Sedimentary Petrology* **40**, 756–758.

SCOFFIN, T.P. 1987. *An Introduction to Carbonate Sediments and Rocks*. Blackie, Glasgow and Hall, New York.

SCOFFIN, T.P. & STODDART, D.R. 1983. Beachrock and intertidal cement. *In:* GOUDIE, A.S. & PYE, K. (eds), *Chemical Sediments and Geomorphology: Precipitates and Residua in the Near-surface Environment*. Academic Press, London, 401–425.

SELLWOOD, B.W. 1995. Principles of carbonate diagenesis. *In:* PARKER, A. & SELLWOOD, B.W. (eds), *Quantitative Diagenesis: Recent Developments and Applications to Reservoir Geology*. NATO ASI Series C: Mathematical and Physical Sciences, 453. Kluwer Academic, Dordrecht, 286.

SPRATT, T.A.B. & FORBES, E. 1847. *Travels in Lycia, Milyas, and the Cibyratis*. II.-John Van Voorst, Paternoster Row, London.

SPURGEON, D., DAVIS JR, R.A. & SHINNU, E.A. 2003. Formation of 'Beach Rock' at Siesta Key, Florida and its influence on barrier island development. *Marine Geology* **200**, 19–29.

STODDART, D.R. & CANN, J.R. 1965. Nature and origin of beachrock. *Journal of Sedimentary Petrology* **35**, 243–247.

SÜMENGEN, M. & TERLEMEZ, İ. 1991. Stratigraphy of Eocene deposits in southwest Trace region. *Mineral Research and Exploration Institute (MTA) Bulletin* **113**, 17–30 [in Turkish with English abstract].

TAYLOR, J.C.M. & ILLING, L.V. 1969. Holocene intertidal calcium carbonate cementation. Qatar, Persian Gulf. *Sedimentology* **12**, 69–107.

TUROĞLU, H. & CÜREBAL, İ. 2005. Karaburun (İstanbul) and Uluabat (Bursa) beachrocks. *Geographical Journal of İstanbul University* **13**, 57–66 [in Turkish with English abstract].

TÜRKEŞ, M. 1996. Spatial and temporal analysis of annual rainfall variations in Turkey. *International Journal of Climatology* **16**, 1057–1076.

VERRECCHIA, E.P. & VERRECCHIA, K. 1994. Needle-fiber calcite: a critical review and a proposed classification. *Journal of Sedimentary Research A* **64**, 650–664.

VIEIRA, M.M. & DE ROS, L.F. 2007. Cementation patterns and genetic implications of Holocene beachrocks from northeastern Brazil. *Sedimentary Geology* **192**, 207–230.

VOUSDOUKAS, M.I., VELEGRAKIS, A.F. & PLOMARITIS, T.A. 2007. Beachrock occurrence, characteristics, formation mechanism and impacts. *Earth-Science Reviews* **85**, 23–46.

WEBB, G.E., JELL, J.S. & BAKER, J.C. 1999. Cryptic intertidal microbialites in beachrock, Heron Island, Great Barrier Reef: implications for the origin of microcrystalline beachrock cement. *Sedimentary Geology* **126**, 317–334.

Received 08 October 2007; revised typescript received 11 February 2008; accepted 19 February 2008